Formation of a Continuous Mesoporous Silica Film with Fully Aligned Mesochannels on a Glass Substrate

Hirokatsu Miyata*,† and Kazuyuki Kuroda‡,§

Canon Inc., R&D Headquarters, Canon Research Center, 5-1, Morinosato-Wakamiya, Atsugi-shi, Kanagawa, 243-0193, Japan; Department of Applied Chemistry, Waseda University, Ohkubo-3, Shinjuku-ku, Tokyo 169-8555, Japan; and Kagami Memorial Laboratory for Materials Science and Technology, Waseda University, Nishiwaseda-2, Shinjuku-ku, Tokyo 169-0051, Japan

Received August 6, 1999

A continuous mesoporous silica film with uniaxially aligned hexagonal mesochannels was formed on a silica glass substrate using a rubbing-treated thin polyimide coating on the substrate. Polyimide which has a hexamethylene group per the repeating unit as a part of the main chain was used. The mesostructured silica film was grown on the polyimide-coated substrate through the hydrolysis of tetraethoxysilane under acidic conditions in the presence of hexadecyltrimethylammonium chloride. X-ray diffraction experiments show that the hexagonal mesochannels in the film run parallel to the substrate surface and are aligned normal to the rubbing direction with a very narrow distribution of ±6°. The hexagonal arrangement of the mesochannels over the whole film thickness was proved by cross-sectional transmission electron microscopy. This highly preferred alignment of the mesochannels is caused by strong interactions between the surfactant tail groups and the polymer chains.

Introduction

Nanoscaled structural control of materials is a key technology in material science of next generation. One of the simple and promising strategies to achieve this aim is to incorporate various guest species into host materials with well-ordered nanospaces,[1−3] and novel molecular devices are expected to be developed by this method.[4−12] New mesoporous materials with highly ordered structures[13−18] are suitable for such host materials. However, both macroscopic control of the morphology and microscopic control of the porous structure are indispensable for practical applications to optical and electrical molecular devices.

Many groups have reported on the ordered mesoporous silica with various macroscopic morphologies such as spheres,[19−21] fibers,[22−24] rods,[25,26] and films.[12,27−42] Among these morphologies, continuous thin films on

* To whom correspondence should be addressed. E-mail: hiro@crc.canon.co.jp.
† Canon Inc.
‡ Department of Applied Chemistry, Waseda University.
§ Kagami Memorial Laboratory for Materials Science and Technology, Waseda University.

(1) Alberti, G.; Bein, T. Solid- State Supramolecular Chemistry: Two- and Three-Dimensional Inorganic Networks. *Comprehensive Supramolecular Chemistry*; Elsevier Science: London, UK, 1996; Vol. 7.
(2) Schöllhorn, R. *Chem. Mater.* **1996**, *8*, 1747.
(3) Moller, K.; Bein, T. *Chem. Mater.* **1998**, *10*, 2950.
(4) (a) Dag, Ö.; Kuperman, A.; Ozin, G. A. *Adv. Mater.* **1995**, *7*, 72. (b) Chomski, E.; Dag, Ö.; Kuperman, A.; Coombs, N.; Ozin, G. A. *Chem. Vap. Deposition* **1996**, *2*, 8. (c) Dag, Ö.; Ozin, G. A.; Yang, H.; Reber, C.; Bussière, G. *Adv. Mater.* **1999**, *11*, 474.
(5) (a) Wu, C.-G.; Bein, T. *Chem. Mater.* **1994**, *6*, 1109. (b) Wu, C.-G.; Bein, T. *Science* **1994**, *264*, 1757.
(6) Leon, R.; Margolese, D.; Stucky, G.; Petroff, P. M. *Phys. Rev. B: Condens. Matter* **1995**, *52*, r2285.
(7) Srdanov, V. I.; Alxneit, I.; Stucky, G. D.; Reaves, C. M.; DenBaars, S. P. *J. Phys. Chem. B* **1998**, *102*, 3341.
(8) Tang, Y. S.; Cai, S.; Jin, G.; Duan, J.; Wang, K. L.; Soyez, H. M.; Dunn, B. S. *Appl. Phys. Lett.* **1997**, *71*, 2448.
(9) Agger, J. R.; Anderson, M. W.; Pemble, M. E.; Terasaki, O.; Nozue, Y. *J. Phys. Chem. B* **1998**, *102*, 3345.
(10) Vietze, U.; Krauss, O.; Laeri, F.; Ihlein, G.; Schüth, F.; Limburg, B.; Abraham, M. *Phys. Rev. Lett.* **1998**, *81*, 4628.
(11) Marlow, F.; McGehee, M. D.; Zhao, D.; Chmelka, B. F.; Stucky, G. D. *Adv. Mater.* **1999**, *11*, 632.
(12) Ryoo, R.; Ko, C. H.; Cho, S. J.; Kim, J. M. *J. Phys. Chem. B* **1997**, *101*, 10610.
(13) Yanagisawa, T.; Shimizu, T.; Kuroda, K.; Kato, C. *Bull. Chem. Soc. Jpn.* **1990**, *63*, 988.
(14) Inagaki, S.; Fukushima, Y.; Kuroda, K. *J. Chem. Soc., Chem. Commun.* **1993**, 680.
(15) Kresge, C. T.; Leonowicz, M. E.; Roth, W. J.; Vartuli, J. C.; Beck, J. S. *Nature* **1992**, *359*, 710.
(16) Beck, J. S.; Vartuli, J. C.; Roth, W. J.; Leonowicz, M. E.; Kresge, C. T.; Schmitt,K. D.; Chu, C. T.-W.; Olson, D. H.; Sheppard, E. W.; McCullen, S. B.; Higgins, J. B.; Schlenker, J. L. *J. Am. Chem. Soc.* **1992**, *114*, 10834.
(17) Huo, Q.; Margolese, D. I.; Ciesla, U.; Feng, P.; Gier, T. E.; Sieger, P.; Leon, R.; Petroff, P. M.; Schuth, F.; Stucky, G. D. *Nature* **1994**, *368*, 317.
(18) Huo, Q.; Margolese, D. I.; Ciesla, U.; Demuth, G. D.; Feng, P.; Gier, T. E.; Sieger, P.; Firouzi, A.; Chmelka, B. F.; Schuth, F.; Stucky, G. D. *Chem. Mater.* **1994**, *6*, 1176.
(19) Yang, H.; Vovk, G.; Coombs, N.; Sokolov, I.; Ozin, G. A. *J. Mater. Chem.* **1998**, *8*, 743.
(20) Huo, Q.; Feng, J.; Schüth, F.; Stucky, G. D. *Chem. Mater.* **1997**, *9*, 14.
(21) Grün, M.; Lauer, I.; Unger, K. K. *Adv. Mater.* **1997**, *9*, 254.
(22) Yang, P.; Zhao, D.; Chmelka, B. F.; Stucky, G. D. *Chem. Mater.* **1998**, *10*, 2033.
(23) Huo, Q.; Zhao, D.; Feng, J.; Weston, K.; Buratto, S. K.; Stucky, G. D.; Schacht, S.; Schüth, F. *Adv. Mater.* **1997**, *9*, 974.
(24) Bruinsma, P. J.; Kim, A. Y.; Liu, J.; Baskaran, S. *Chem. Mater.* **1997**, *9*, 2507.
(25) Schmidt-Winkel, P.; Yang, P.; Margolese, D. I.; Chmelka, B. F.; Stucky, G. D. *Adv. Mater.* **1999**, *11*, 303.
(26) Lin, H.-P.; Liu, S.-B.; Mou, C.-Y.; Tang, C.-Y. *Chem. Commun.* **1999**, 583.
(27) (a) Ogawa, M. *J. Am. Chem. Soc.* **1994**, *116*, 7941. (b) Ogawa, M. *Langmuir* **1997**, *13*, 1853.
(28) Ogawa, M. *Chem. Commun.* **1996**, 1149.
(29) Ogawa, M.; Ishikawa, H.; Kikuchi, T. *J. Mater. Chem.* **1998**, *8*, 1783.
(30) Ogawa, M.; Kikuchi, T. *Adv. Mater.* **1998**, *10*, 1077.

10.1021/cm990506k CCC: $19.00
Published on Web 12/21/1999

substrates are particularly important, and the film formations have been achieved by solvent evaporation method[27−30,36−40] and through heterogeneous nucleation at interfaces.[31−35,42]

On the other hand, the alignment of the mesochannels is also an important issue. Preferred alignment of the mesochannels is achieved using regular atomic arrangements on crystalline surfaces.[31−34,42] The cleaved surfaces of mica[31] and graphite[32,33] provide a partial alignment, and silicon (110) surface[42] provides a whole alignment of the mesochannels in the mesostructured silica films grown on these substrates. However, the restriction of the applicable substrates obstructs wider applications of the mesoporous silica films. Therefore, methods to align the mesochannels on conventional substrates such as glass plates have been desired.

A flow-induced alignment is one of the candidates for the alignment of the mesochannels. Preferred alignment of mesoporous silica has been reported using a continuous-flow[43,44] and an electroosmotic flow within microcapillaries on a substrate.[45] Although the alignment was achieved, these methods require special apparatus and restrict the applicable substrates. Zhao et al. reported that the alignment of the mesochannels in the film was achieved through a dip coating.[39] However, the templating materials used in their experiments were limited to specialized nonionic surfactants such as block copolymers, and the direct evidence of the whole alignment of the mesochannels in the film was not clearly presented.

Recently, we reported that a rubbing-treated polyimide film formed on a glass substrate provides a preferred alignment of the mesochannels in the mesoporous silica parallel to the rubbing direction.[46] However, the mesoporous silica on the substrate was not a continuous film but a discrete parallel arrangement of the elongated mesoporous silica particles. In this article, we report a successful formation of a continuous mesoporous silica film with fully aligned mesochannels. The alignment over the whole film thickness was proved by in-plane X-ray diffraction (XRD) and cross-sectional transmission electron microscopy (TEM). The continuity of the mesoporous silica film and the alignment direction of the mesochannels strongly depend on the chemical structure of the polyimide. By using a polyimide that has nonbranched aliphatic parts in the main chain, we obtained a continuous mesoporous silica film in which the hexagonal mesochannels run perpendicular to the rubbing direction.

Experimental Section

A polyimide precursor, polyamic acid, was spin-coated onto a clean silica glass substrate and baked at 200 °C for 1 h in air atmosphere to convert into a polyimide film.[47] The ideal structure of the polyimide is shown in the top of Figure 1a. This polyimide is abbreviated as PI-1 hereafter. The thickness of the polyimide film was about 10 nm as determined by ellipsometry. The polyimide film on the substrate was rubbing-treated using a nylon-covered cylindrical roller (buffing wheel) of 24-mm radius. The polyimide-coated substrate was fixed on a height-controllable stage which linearly moves toward the buffing wheel with controlled velocity. The intensity of the rubbing treatment is controlled by rotational speed of the buffing wheel, velocity of the stage, and pressing intensity of the buffing wheel to the substrate surface. For the typical rubbing conditions, the rotational speed was 1000 rpm, stage velocity was 600 mm/min, and the substrate was pressed by 0.4−0.5 mm to the buffing wheel. The rubbing treatment was repeated two times. All the polyimide films used in this report were prepared according to the same procedure and rubbing-treated under the same conditions.

The mesostructured silica film formation was performed through the hydrolysis of silicon alkoxide in the presence of surfactants under the acidic conditions as reported by Yang et al.[31] TEOS (tetraethoxysilane, $(C_2H_5O)_4Si$) was mixed with an acidic cationic surfactant CTACl (hexadecyltrimethylammonium chloride, $CH_3(CH_2)_{15}N(CH_3)_3Cl$) solution and the mixture was stirred for 2.5 min at room temperature and transferred into a Teflon vessel. The molar ratio was 0.10 TEOS:0.11 CTACl:100 H_2O:7.0 HCl. The substrate described above was held horizontally in the mixture using a substrate holder with the rubbed polyimide surface downward. The surface of the substrate was covered with another silica glass with a ∼0.2 mm spacing in order to obtain a uniform film. The vessel was sealed and held at 80 °C for 1 week for the formation of the mesoporous silica film. After the reaction, the as-synthesized film was washed with distilled water and dried in air. The calcination of the sample was conducted under an air atmosphere in a muffle furnace at 540 °C for 10 h at a rate of 2 °C min^{-1}.

The morphology of the sample was observed with an optical microscope (Olympus BH2). The mesoporous structure was elucidated by XRD (Rigaku RAD-2R) using Cu Kα radiation with a graphite monochromator. A grazing angle in-plane XRD study[48] was performed on a X-ray diffractometer equipped with a four-axes goniometer (Rigaku ATX-G) with a parabolic multilayer mirror as primary beam condenser. Cu Kα radiation from a copper rotating anode was used for the experiment. The incident angle of X-rays, α, was set to 0.2°. Transmission electron microscopic images were recorded on an Akashi 002B microscope at an accelerating voltage of 100 kV. The specimen for the cross-sectional TEM observation was prepared as follows: first, the sample was embedded in an epoxy resin and was sawed into a piece with a thickness of ∼500 μm; second, the piece was mechanically prethinned and polished by a disk grinder and a dimple grinder to produce a central region of

(31) Yang, H.; Kuperman, A.; Coombs, N.; Mamiche-Afara, S.; Ozin, G. A. *Nature* **1996**, *379*, 703.
(32) Aksay, I. A.; Trau, M.; Manne, S.; Honma, I.; Yao, N.; Zhou, L.; Fenter, P.; Eisenberger, P. M.; Gruner, S. M. *Science* **1996**, *273*, 892.
(33) Yang, H.; Coombs, N.; Sokolov, I.; Ozin, G. A. *J. Mater. Chem.* **1997**, *7*, 1285.
(34) Coombs, N.; Khushalani, D.; Oliver, S.; Ozin, G. A.; Shen, G. C.; Sokolov, I.; Yang, H. *J. Chem. Soc., Dalton Trans.* **1997**, 3941.
(35) Tolbert, S. H.; Schäffer, T. E.; Feng, J.; Hansma, P. K.; Stucky, G. D. *Chem. Mater.* **1997**, *9*, 1962.
(36) Martin, J. E.; Anderson, M. T.; Odinek, J.; Newcomer, P. *Langmuir* **1997**, *13*, 4133.
(37) Lu, Y.; Ganguli, R.; Drewien, C. A.; Anderson, M. T.; Brinker, C. J.; Gong, W.; Guo, Y.; Soyez, H.; Dunn, B.; Huang, M. H.; Zink, J. I. *Nature* **1997**, *389*, 364.
(38) Zhao, D.; Yang, P.; Margolese, D. I.; Chmelka, B. F.; Stucky, G. D. *Chem. Commun.* **1998**, 2499.
(39) Zhao, D.; Yang, P.; Melosh, N.; Feng, J.; Chmelka, B. F.; Stucky, G. D. *Adv. Mater.* **1998**, *10*, 1380.
(40) Ko, C. H.; Kim, J. M.; Ryoo, R. *Microporous Macroporous Mater.* **1998**, *21*, 235.
(41) (a) Yang, H.; Coombs, N.; Sokolov, I.; Ozin, G. A. *Nature* **1996**, *381*, 589. (b) Yang, H.; Coombs, N.; Dag, Ö.; Sokolov, I.; Ozin, G. A. *J. Mater. Chem.* **1997**, *7*, 1755. (c) Yang, H.; Ozin, G. A.; Kresge, C. T. *Adv. Mater.* **1998**, *10*, 883.
(42) Miyata, H.; Kuroda, K. *J. Am. Chem. Soc.* **1999**, *121*, 7621.
(43) Hillhouse, H. W.; Okubo, T.; van Egmond, J. W.; Tsapatsis, M. *Chem. Mater.* **1997**, *9*, 1505.
(44) Hillhouse, H. W.; van Egmond, J. W.; Tsapatsis, M. *Langmuir* **1999**, *15*, 4544.
(45) Trau, M.; Yao, N.; Kim, E.; Xia, Y.; Whitesides, G. M.; Aksay, I. A. *Nature* **1997**, *390*, 674.
(46) Miyata, H.; Kuroda, K. *Chem. Mater.* **1999**, *11*, 1609.
(47) Mittal, K. L. *Polyimides*; Plenum Press: New York, 1984.
(48) Marra, W. C.; Eisenberger, P.; Cho, A. Y. *J. Appl. Phys.* **1979**, *50*, 6927.

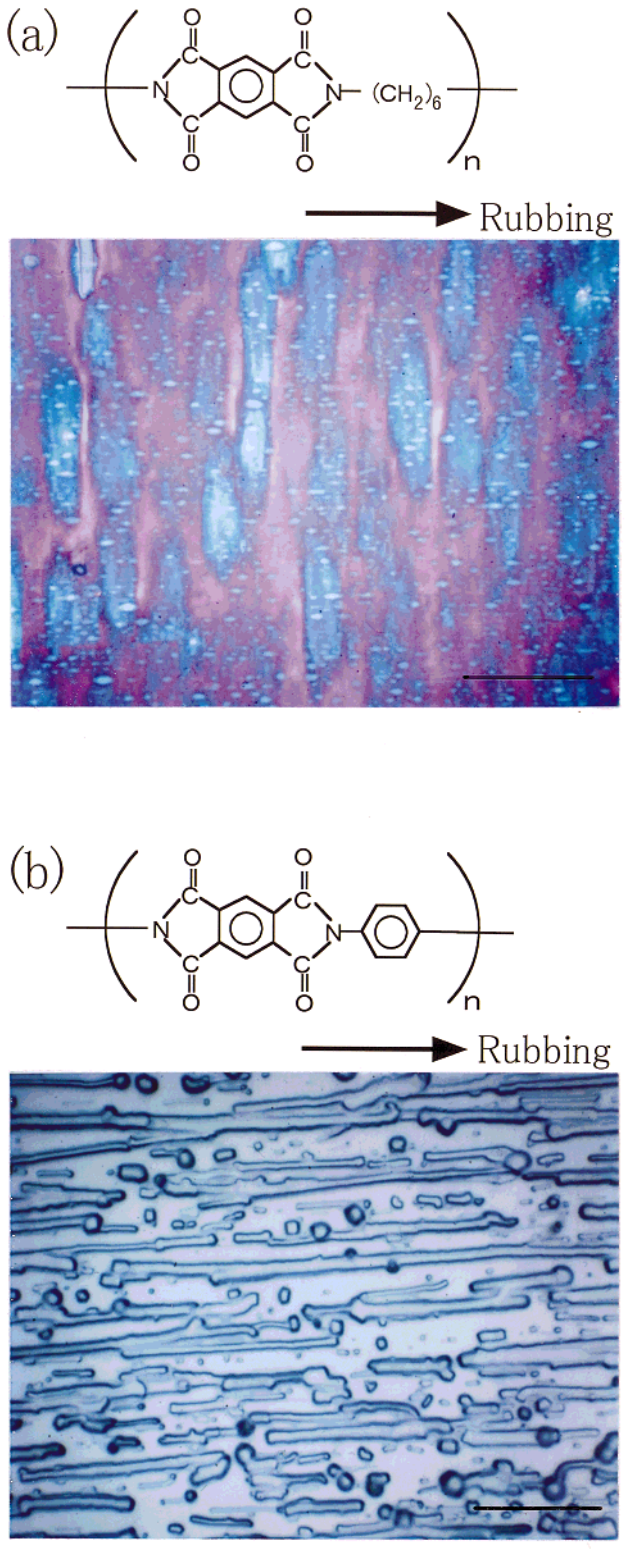

Figure 1. The ideal structure of the polyimides (top) and the optical microscopic images of the as-grown mesostructured silica films on each rubbing-treated polyimide film (bottom): (a) PI-1 and (b) PI-2. Arrows show the rubbing directions. Scale bar: 20 μm.

$\sim$10 μm thick; and finally, the central region was milled with two Ar^+ ion beams of 3 keV energy with incident angles $-1°$ and 4°, respectively.

Results and Discussion

A glossy continuous film with a 0.3−0.5-μm thickness was formed on the rubbing-treated PI-1 film coated on a silica glass substrate. The optical microscopic image (reflection) of the as-grown film is shown in Figure 1a. For the comparison, the structure of the polyimide used in the previous study,[46] abbreviated as PI-2, and the microscopic image of the as-grown mesostructured silica on it is shown in Figure 1b. PI-1 has a hexamethylene group per the repeating unit instead of a phenylene group of PI-2 to provide a more hydrophobic surface.

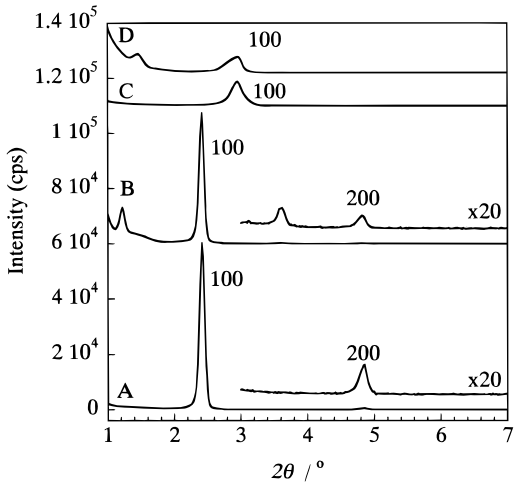

Figure 2. XRD profiles ($\theta - 2\theta$ scanning) obtained for the mesostructured silica film grown on the rubbing-treated PI-1 film: (A) as-grown film, recorded for the geometry of X-rays parallel to the rubbing direction; (B) as-grown film, X-rays perpendicular to the rubbing direction; (C) calcined film, X-rays parallel to the rubbing direction; and (D) calcined film, X-rays perpendicular to the rubbing direction.

In Figure 1a, preferred alignment of ellipsoid-shaped texture was observed perpendicular to the rubbing direction. Similar textures are also observable in the continuous mesostructured film formed on mica[31] and silicon (110) surfaces,[42] indicating a preferred alignment of the mesostructured silica. The observed texture is caused by a different interference color due to a slight difference of the film thickness within a continuous film, and does not show a discrete film structure. The mesoporous silica formed on the rubbing-treated PI-2 film has a discrete morphology (Figure 1b) as reported previously.[46]

The mesoscopic structure of the film grown on the rubbing-treated PI-1 film was confirmed by XRD. The conventional $\theta - 2\theta$ scanning XRD patterns are shown in Figure 2. The trace A is a scanning profile of the as-grown film when the rubbing direction of the sample was set parallel to the incident X-rays at $\theta = 0°$. Two diffraction peaks assigned as (100) and (200) of the hexagonal structure were observed at $2\theta = 2.4°$ ($d_{100} =$ 3.6 nm) and 4.8°($d_{200} = 1.8$ nm), respectively. The lack of (110) diffraction peak shows that the mesochannels run parallel to the substrate surface as has been already demonstrated in other mesostructured films.[31,33] When the rubbing direction of the sample was set normal to the incident X-rays at $\theta = 0°$, two additional diffraction peaks were observed at $2\theta = 1.2°$ ($d = 7.2$ nm) and 3.6° ($d = 2.4$ nm), as shown in the trace B. The difference of the XRD patterns measured from the two directions indicates the anisotropic arrangement of the mesochannels in the mesostructured silica film. The lattice spacings of these two additional diffraction peaks are exactly 2 and $^2/_3$ times of the d_{100} value, and these peaks

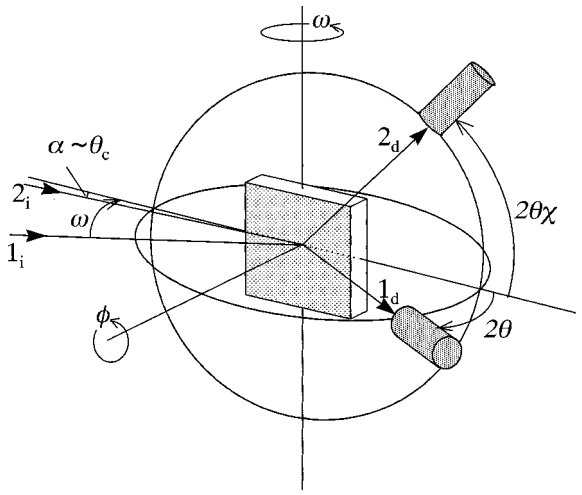

Figure 3. The geometry of the in-plane diffraction and the four axes of the goniometer. 1_i and 1_d represent the incident and diffracted X-ray paths for the conventional XRD, whereas 2_i and 2_d represent the incident and diffracted X-ray paths for the in-plane XRD. ω and 2θ are the rotation axes of the sample and the detector for the conventional XRD, whereas ϕ and $2\theta\chi$ are the rotation axes of the sample and the detector for the in-plane XRD.

should be forbidden reflections for a perfect hexagonal channel structure under ideal measurement conditions. The appearance of these additional diffraction peaks only for the geometry of X-rays normal to the rubbing direction can be explained by the vertical divergence of the incident X-rays (~5° in this experimental setup) and strong anisotropy of the arrangement of the hexagonally packed mesochannels in the film. The detailed explanation about the correspondence between the anisotropic mesochannel arrangement and the obtained XRD patterns will be reported shortly.

The morphology of the film was not changed, at least for the optical microscopic scales, after the removal of the surfactant by calcination, and no cracks were induced. The traces C and D in Figure 2 show the XRD patterns of the calcined film. These patterns were recorded for the sample geometry where the rubbing direction was set parallel (C) and normal (D) to the incident X-rays at $\theta = 0°$, respectively. Although the diffraction intensity was considerably decreased, the existence of the characteristic diffraction peaks of the hexagonal structure shows the reservation of the mesostructure. The anisotropic structural feature of the film is also maintained. The observed peak shift toward the higher 2θ positions and the decrease of the diffraction intensities were caused by the condensation of residual hydroxyl groups in the wall over the calcination.

In-plane XRD study was conducted to obtain a direct evidence of the uniaxial alignment of the mesochannels over the whole film. The direct evidence for the alignment of the mesochannels in the film is not available using conventional $\theta - 2\theta$ measurements because only the structural information parallel to the film surface is obtainable. In-plane X-ray diffraction is caused by the lattice planes normal to the film surface when the X-rays are impinged to the sample surface at a grazing angle around the total reflection angle (θc).[48] The geometry of the in-plane diffraction and the four axes of the goniometer are illustrated in Figure 3. The incident and diffracted X-ray paths for the in-plane XRD measurement are shown as 2_i and 2_d in Figure 3.

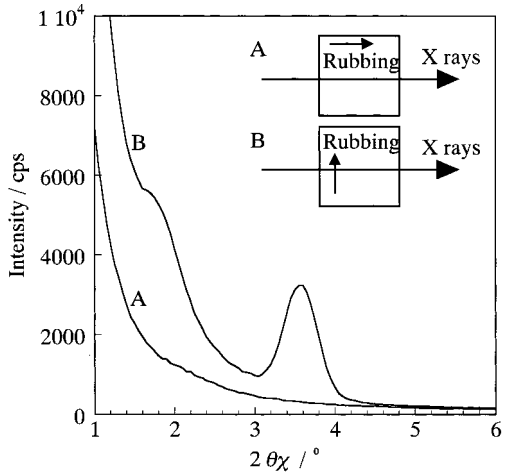

Figure 4. $\phi - 2\theta\chi$ scan profiles of in-plane XRD obtained for the as-grown mesostructured silica film on the rubbing-treated PI-1 film: (A) the rubbing direction is set parallel and (B) normal to the incident X-rays at $\phi = 0°$. Inset: Schematic illustrations of sample orientation to incident X-rays.

The $\phi - 2\theta\chi$ scanning profiles of the as-grown film are shown in Figure 4. Traces A and B were recorded with the sample orientations that the rubbing direction of the polyimide was set parallel and normal to the direction of the incident X-rays at $\phi = 0°$, respectively. In the trace B, a diffraction peak is observed at $2\theta\chi = 3.58°$, corresponding to the lattice spacing of 2.47 nm. This peak was assigned to be (110) on the basis of the mesochannel arrangement deduced from the fact that the (110) peak is not observed in the conventional $\theta - 2\theta$ XRD pattern.[46] The broad shoulder around 1.7° is assigned to be ($^1/_2$ $^1/_2$ 0) from the estimated lattice spacing. The lattice spacing of (110) is larger than the expected value from the d_{100} obtained by conventional XRD, indicating the hexagonal channel structure is distorted. The deviation from the ideal hexagonal channel structure is estimated to be 18%, indicating a larger distortion of the mesoporous silica film than those on mica and silicon (110).[32,42] In contrast to the trace B, no diffraction peaks were observed in trace A, indicating a strong anisotropy of the channel structure.

For the quantitative estimation of the distribution of the mesochannel orientation, a ϕ-scan was conducted fixing the detector position ($2\theta\chi$) at the (110) diffraction peak maximum (3.58°). The rubbing direction of the sample was set parallel to the incident X-rays at $\phi = 0°$. The ϕ-scan profile of the as-grown film is shown in Figure 5. Two sharp diffraction peaks were observed with an interval of 180°. From the peak positions, the alignment direction is proved to be perpendicular to the rubbing direction. This result confirms the full alignment of the mesochannels with a very narrow directional distribution. The ϕ-scan profile can be Gaussian-fitted, indicating the mesochannel orientation shows a Gaussian-type distribution. The full width at half-maximum (fwhm) of the Gaussian distribution was determined to be 12.6°. This distribution is much narrower than that observed on a Si (110) substrate.[42]

The alignment of the mesochannels in the film is also evidenced by the cross-sectional TEM observation. Figure 6 is the cross-sectional TEM image of the as-synthesized mesostructured silica film grown on the

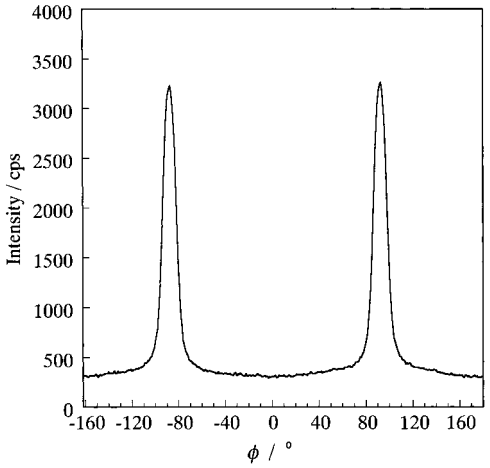

Figure 5. ϕ scan profile of in-plane XRD obtained for the as-grown mesostructured silica film on the rubbing-treated PI-1 film. Rubbing direction is set parallel to the incident X-rays at $\phi = 0°$. The position of the detector is set at the (110) diffraction peak maximum for the $\phi - 2\theta\chi$ scan profile (3.58°).

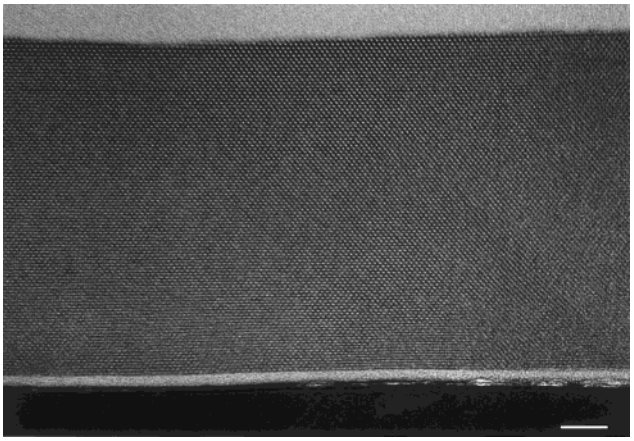

Figure 6. Cross-sectional TEM image of the as-synthesized mesostructured silica film grown on the rubbing-treated PI-1 film. The image was recorded at an accelerating voltage of 100 kV (scale bar: 50 nm). The sample was sliced perpendicular to the long axes of the mesoporous silica domains.

rubbing-treated PI-1 film sliced perpendicular to the long axes of the mesoporous silica domains. The hexagonal mesoporous structure was clearly observed over all thicknesses of the film, showing a complete alignment of the mesochannels. The distortion of the hexagonal packing is also confirmed by an high-magnification TEM image (not shown).

In this report, we proved that the alignment and morphology of the mesostructured silica grown on a rubbing-treated substrate strongly depend on the molecular structure of the surface coating. The mesostructured silica grown on a rubbing-treated PI-2 film was not a continuous film and many round-shaped particles were observed along the elongated particles (Figure 1b). On the other hand, no such particles were grown on a rubbed PI-1 film and the surface was fully covered by the mesostructured silica. This difference should be largely ascribed to the difference of the hydrophobicity between these two polyimide films. PI-1 has a hydrophobic hexamethylene group per the repeating unit, which provides a large interaction area with the surfactant molecules. Perhaps this strong hydrophobic interaction increases the number of the nucleation site

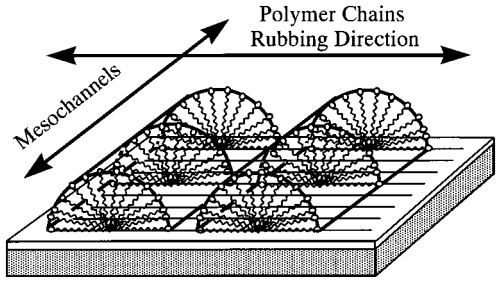

Figure 7. Schematic illustration of the alignment of surfactants and mesochannels on the rubbing-treated PI-1 film.

and promotes the growing of each silicate−surfactant seed.

In addition to the hydrophobicity of the surface, the susceptibility for the rubbing treatment is considered to be an important factor. Since the chemical structure of PI-2 consists of rings, the polymer chain of PI-2 is hard to be expanded by the rubbing treatment, whereas PI-1 contains flexible hexamethylene groups and easy to be expanded to the rubbing direction. The unidirectional expansion of the polymer chain leads to the alignment of the polymer chains, which enables surfactant molecules to accommodate parallel to the polymer chain through the hydrophobic interactions. The strong molecular-level interactions between the aligned hexamethylene part of the polymer chain and the tail group of the surfactant make the mesochannels align perpendicular to the rubbing direction as schematically shown in Figure 7. For PI-2, the effect of rubbing on the alignment of the polymer chain is considered to be small because of the stiff chemical structure. Although mesostructured silica particles align parallel to the rubbing direction on the rubbing-treated PI-2 film, we have found, very recently, that they align perpendicular to the axes of the polymer chains on a PI-2 Langmuir−Blodgett (LB) film.[49] In the PI-2 LB film, the polymer chains are proved to be oriented along the withdrawal direction of the substrate during the LB film deposition. These two different alignment directions on the same polymer indicate that the rubbing-induced orientation of the polymer chains in the rubbing-treated PI-2 film is not enough to align mesostructured silica through molecular-scaled interactions between the polymer chain and the surfactant. Alignment mechanisms other than molecular-scaled interactions, for example a morphological effect induced by microgrooves on the rubbed surface, should contribute to the alignment on the rubbing-treated PI-2 film. However, because an SiO obliquely evaporated film does not provide the alignment of mesoporous silica, as we have already shown,[46] the alignment should not be provided only by a morphological effect. The alignment mechanism on the rubbing-treated PI-2 film is still ambiguous.

Another important requirement for the polymer which provides a good uniaxial alignment of mesostrustured silica is a linearity of the structure. It means both straight main polymer chains and the absence of side chains. This requirement is also applied to the alignment of thermotropic liquid crystals,[50] where the linear polymers tend to provide good alignment after a rubbing

(49) Miyata, H.; Kuroda, K. *Adv. Mater.* **1999**, *11*, 1448.
(50) Fukuda, A.; Takezoe, H. *Structures and properties of ferroelectric liquid crystals*; Corona Publishing: Tokyo, 1990.

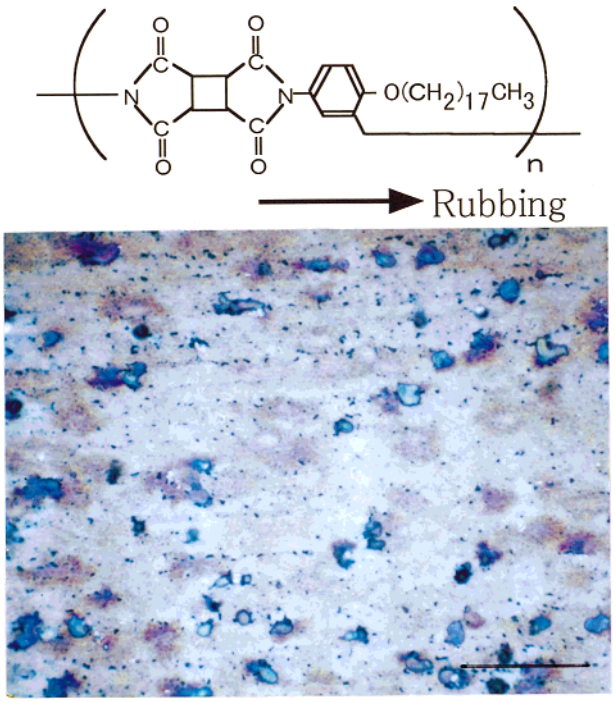

Figure 8. The ideal structure of PI-3 (top) and the optical microscopic image of the as-grown mesostructured silica film on the rubbing-treated PI-3 film (bottom). Arrow shows the rubbing direction. Scale bar: 20 μm.

treatment. As a reference experiment, we used a rubbing-treated nonlinear polyimide (PI-3) film for the growth of the mesostructured film. The structure of PI-3 is shown in the top of Figure 8. PI-3 has a folded main chain structure and has a long alkyl group per the repeating unit as a side chain. In the optical microscopic scale, a continuous mesostructured silica film was formed on the PI-3 film as expected from the hydrophobicity of PI-3. However, the image of the optical microscope (Figure 8, bottom) implies that the alignment direction of the mesochannels is parallel to the rubbing direction unlike the alignment on the PI-1 film. Besides, many round-shaped particles are observed in the film, indicating an inferior alignment. These were proved by in-plane XRD. The ϕ-scan profile of the (110) diffraction intensity is shown in Figure 9a. Although a periodic variation of the diffraction intensity proves the alignment of the mesochannels in the film along the rubbing direction, the distribution is very broad with the fwhm of 72°. Moreover, a weak (110) diffraction peak was still observed in a $\phi - 2\theta\chi$ scanning profile measured with the geometry that the rubbing direction of the polyimide was set normal to the direction of the incident X-rays at $\phi = 0°$ (Figure 9b, trace B). These results clearly show the weak alignment effect of PI-3 which has a nonlinear structure.

Conclusion

We have succeeded in forming a continuous hexagonal mesoporous silica film with fully aligned mesochannels on a glass substrate using a rubbing-treated linear polyimide which has a hexamethylene group per the repeating unit. The distribution of the direction of the

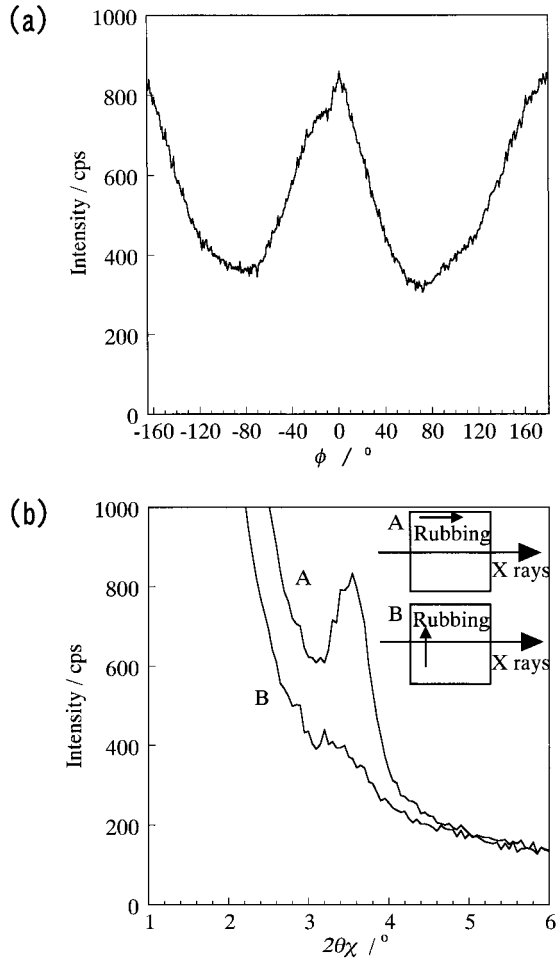

Figure 9. (a) ϕ scan profile of in-plane XRD obtained for the as-grown mesostructured silica film on the rubbing-treated PI-3 film. The rubbing direction is set parallel to the incident X-rays at $\phi = 0°$. The position of the detector is set at the (110) diffraction peak maximum for the $\phi - 2\theta\chi$ scan profile (3.55°). (b) $\phi - 2\theta\chi$ scan profiles of in-plane XRD obtained for the as-grown mesostructured silica film on the rubbing-treated PI-3 film. (A) The rubbing direction is set parallel, and (B) normal to the incident X-rays at $\phi = 0°$. Inset: schematic illustrations of sample orientation to incident X-rays.

mesochannels was very narrow, showing strong interactions between the surface polymer chains and the surfactant molecules. We propose that the requirements for the polymer which provides a good uniaxial alignment of the mesostructured silica by a rubbing method are hydrophobicity, susceptibility for the rubbing treatment, and the linearity of the polymer structure. This method can be applied to many substrates other than glass, such as metals and semiconductors. This uniaxially oriented continuous mesoporous silica film will find many applications for optical and electronic devices.

Acknowledgment. The authors acknowledge Dr. K. Inaba (Rigaku Co. X-ray Research Laboratory) for the in-plane X-ray diffraction measurement. The authors also acknowledge Mr. T. Noma and Mr. M. Watanabe (Canon Inc., Canon Research Center) for useful discussion on XRD results and cross-sectional TEM observation.

CM990506K